THE JOURNAL OF BIOLOGICAL CHEMISTRY VOL. 285, NO. 20, pp. 15430–15439, May 14, 2010

Acute Modulation of Sugar Transport in Brain Capillary Endothelial Cell Cultures during Activation of the Metabolic Stress Pathway*[S]

Received for publication, February 3, 2010, and in revised form, March 11, 2010 Published, JBC Papers in Press, March 15, 2010, DOI 10.1074/jbc.M110.110593

Anthony J. Cura and Anthony Carruthers[1]

From the Department of Biochemistry and Molecular Pharmacology, University of Massachusetts Medical School, Worcester, Massachusetts 01605

GLUT1-catalyzed equilibrative sugar transport across the mammalian blood-brain barrier is stimulated during acute and chronic metabolic stress; however, the mechanism of acute transport regulation is unknown. We have examined acute sugar transport regulation in the murine brain microvasculature endothelial cell line bEnd.3. Acute cellular metabolic stress was induced by glucose depletion, by potassium cyanide, or by carbonyl cyanide *p*-trifluoromethoxyphenylhydrazone, which reduce or deplete intracellular ATP within 15 min. This results in a 1.7–7-fold increase in V_{max} for zero-trans 3-*O*-methylglucose uptake (sugar uptake into sugar-free cells) and a 3–10-fold increase in V_{max} for equilibrium exchange transport (intracellular [sugar] = extracellular [sugar]). GLUT1, GLUT8, and GLUT9 mRNAs are detected in bEnd.3 cells where GLUT1 mRNA levels are 33-fold greater than levels of GLUT8 or GLUT9 mRNA. Neither GLUT1 mRNA nor total protein levels are affected by acute metabolic stress. Cell surface biotinylation reveals that plasma membrane GLUT1 levels are increased 2–3-fold by metabolic depletion, although cell surface Na^+,K^+-ATPase levels remain unaffected by ATP depletion. Treatment with the AMP-activated kinase agonist, AICAR, increases V_{max} for net 3-*O*-methylglucose uptake by 2-fold. Glucose depletion and treatment with potassium cyanide, carbonyl cyanide *p*-trifluoromethoxyphenylhydrazone, and AICAR also increase AMP-dependent kinase phosphorylation in bEnd.3 cells. These results suggest that metabolic stress rapidly stimulates blood-brain barrier endothelial cell sugar transport by acute up-regulation of plasma membrane GLUT1 levels, possibly involving AMP-activated kinase activity.

The cells of the mammalian brain do not contain large stores of glycogen. It is therefore essential that glucose uptake by the brain exceeds glucose utilization to maintain proper brain function. To enter the brain, serum glucose must cross the blood-brain barrier, an epithelium comprising endothelial cells connected by tight junctions that prevent paracellular diffusion of glucose and other nutrients. Thus, glucose transport into the brain requires trans-endothelial cell transport. This process is catalyzed by the glucose transport protein GLUT1, which is expressed at both luminal and abluminal membranes of the endothelium (1–5).

Endothelial cells of the blood-brain barrier (bEND)[2] differ from those of the peripheral circulatory system (pEND) in several important ways. 1) bEND cells contain 2–5-fold more mitochondria than pEND cells (6). 2) Brain capillary walls (comprising bEND cells) are 40% thinner than capillary walls of the peripheral circulation (7). 3) pEND cells present significantly fewer tight junctions than bEND cells (8). 4) bEND cell tight junction complexes result in polarized cell surface protein expression that is less marked or absent in pEND cells (8). The resulting bEND cell architecture may give rise to behaviors that differ from those of pEND cells but that resemble those of other metabolically active cells and thereby optimally support blood-brain barrier physiology (*e.g.* transport sensitivity to loss of cellular oxidative metabolic capacity).

Although a simple equilibrative process, GLUT1-mediated trans-endothelial cell sugar transport appears to be tightly regulated. Sugar transport into the brain only narrowly exceeds brain glucose utilization under normal conditions (9). Under conditions of metabolic stress, such as hypoxia (10), hypoglycemia (11–13), and seizures (14, 15), the glucose import capacity of the brain is up-regulated. Endothelial cell affinity for transported sugars appears to be unchanged (15). There are three possible explanations for increased V_{max} for transport as follows: 1) increased GLUT1 at the plasma membrane, either through increased protein expression or recruitment of intracellular stores; 2) enhanced intrinsic activity of GLUT1, which catalyzes faster translocation of substrate through the carrier, as seen in the ATP modulation of GLUT1 in erythrocytes (16–20); or 3) a combination of both effects.

Chronic stress induces transcriptional up-regulation of endothelial GLUT1 levels *in vitro* (21) and *in vivo* (22). Although increased protein expression could account for acute stimulation of sugar transport, immunogold staining of cells during

* This work was supported, in whole or in part, by National Institutes of Health Grants DK 36081 and DK 44888.

[S] The on-line version of this article (available at http://www.jbc.org) contains supplemental Fig. 1.

[1] To whom correspondence should be addressed: 364 Plantation St., LRB Rm. 926, Worcester, MA 01605. Tel.: 508-856-5570; Fax: 508-856-6464; E-mail: anthony.carruthers@umassmed.edu.

[2] The abbreviations used are: bEND, endothelial cells of the blood-brain barrier; pEND, endothelial cells of the peripheral circulatory system; KCN, potassium cyanide; FCCP, carbonyl cyanide *p*-trifluoromethoxyphenylhydrazone; DMEM, Dulbecco's modified Eagle's medium; PBS, phosphate-buffered saline; DPBS, Dulbecco's phosphate-buffered saline; AMPK, AMP-activated protein kinase; RT, reverse transcriptase; BisTris, 2-[bis(2-hydroxyethyl)amino]-2-(hydroxymethyl)propane-1,3-diol; MES, 4-morpholineethanesulfonic acid; 3-OMG, 3-*O*-methylglucose; AICAR, 5-aminoimidazole-4-carboxamide-1-β-D-ribofuranosyl monophosphate.

seizures has not conclusively demonstrated altered cellular GLUT1 content (23).

Between 30 and 50% of total cellular GLUT1 resides in cytosolic vesicles in endothelial cells (24). GLUT1 recruitment to the plasma membrane occurs in response to acute metabolic stress in rat liver epithelial cells *in vitro* (25) and in response to growth factor stimulation in bovine retinal endothelial cells (26). We therefore set out to examine whether cultured brain microvessel endothelial cells respond to acute metabolic stress with increased sugar transport capacity and, if so, to test the hypothesis that increased V_{max} for sugar uptake results from recruitment of intracellular GLUT1 to the plasma membrane. Using the mouse brain microvascular endothelial cell line bEnd.3 (27), we have determined the steady-state kinetics of GLUT1-mediated sugar transport in the absence and presence of glucose or the metabolic poisons potassium cyanide (KCN) and carbonyl cyanide *p*-trifluoromethoxyphenylhydrazone (FCCP). We established conditions for bEnd.3 cell ATP depletion, measured total GLUT1 mRNA and protein levels, and measured changes in plasma membrane levels of GLUT1. We show that ATP depletion of bEnd.3 cells increases V_{max} for sugar transport and increases plasma membrane GLUT1 levels without changing endothelial cell GLUT1 mRNA or total GLUT1 protein levels. We also show that glucose depletion and treatment with KCN and FCCP increase the phosphorylation of the AMP-activated protein kinase AMPK. Treatment of bEnd.3 cells with the AMPK agonist AICAR increases both the V_{max} for sugar transport and the phosphorylation of AMPK. Taken together, these data suggest a potential role for AMPK in regulating the acute endothelial cell response to metabolic stress.

EXPERIMENTAL PROCEDURES

Tissue Culture—bEnd.3 cells were obtained from ATCC and maintained in Dulbecco's modified Eagle's medium (DMEM) (Invitrogen) supplemented with 10% fetal bovine serum (Hyclone) and 1% penicillin/streptomycin solution (Invitrogen) at 37 °C in a humidified 5% CO_2 incubator. All experiments were performed at cell confluence. Plates were subcultured at a ratio of 1:2–1:3 by washing with sterile Dulbecco's phosphate-buffered saline (DPBS) and treating with 0.5% trypsin/EDTA (Invitrogen) for 5–7 min at 37 °C. Passages 3–16 were used in all experiments.

Antibodies—A custom-made affinity-purified rabbit polyclonal antibody raised against a synthetic peptide corresponding to GLUT1 amino acids 480–492 was produced by New England Peptide. A mouse monoclonal antibody against Na^+,K^+-ATPase was purchased from Abcam. Rabbit polyclonal and monoclonal antibodies against AMPK and phosphorylated AMPK were obtained from Cell Signaling Technology. Horseradish peroxidase-conjugated goat anti-rabbit and goat anti-mouse secondary antibodies were obtained from the Jackson Laboratory.

Buffers—Cell Lysis Buffer consisted of 5 mM HEPES, 5 mM $MgCl_2$, 150 mM NaCl, 50 μM EDTA, and 1% SDS. Uptake stop solution included 10 μM cytochalasin B (Sigma) and 100 μM phloretin (Sigma) in DPBS. TAE Buffer consisted of 40 mM Trizma base, 1 mM EDTA, and 20 mM acetic acid. TBS consisted of 20 mM Tris base and 135 mM NaCl, pH 7.6. TBST consisted of TBS Buffer with 0.2% Tween 20. Biotin Quench solution consisted of 250 mM Trizma Base. Biotin Lysis Buffer consisted of TBS with 0.5% Triton X-100.

End Point Reverse Transcriptase-PCR (RT-PCR)—Confluent bEnd.3 cells were washed with DPBS and then incubated with either DPBS, DPBS + 5 mM KCN, or DPBS + 8 μg/ml FCCP (Sigma). Cells were incubated for 10 min at 37 °C and washed twice with DPBS. Total RNA was isolated from bEnd.3 cells using the RNeasy mini kit and QIAshredder (Qiagen). Reverse transcriptase-PCR was carried out on bEnd.3 RNA samples using One-Step RT-PCR kit (Qiagen) as per instructions using the following primers (IDT): GLUT1, 5′-GAACCTGTTGGCCTTTGTGGC-3′ and 5′-GCTGGCGGTAGGCGGGTGAGCG-3′, which produced a DNA fragment of 515 bp; GLUT2, 5′-AAGAGGAGACTGAAGGATCTGC-3′ and 5′-GTAGCAGACACTGCAGAAGAGC-3′, which produced a DNA fragment of 461 bp (28); GLUT3, 5′-CGCCGTGACTGTTGCCACGATC-3′ and 5′-CCACAGTTCTTCAGAGCCCAGA-3′, which produced a DNA fragment of 517 bp; GLUT4, 5′-TGCAACGTGGCTGGGTAGGCAA-3′ and 5′-AGGGAGTACTGTGAGAGCCAGA-3′, which produced a DNA fragment of 444 bp; GLUT5, 5′-CTAACTGGAGTCCCCGCAGGCC-3′ and 5′-GACACAGACAATGCTGATATAG-3′, which produced a DNA fragment of 548 bp; GLUT6, 5′-ACCCCCTGATGTTCGTGGGGCC-3′ and 5′-CGTAGAGCCCCAGTGTCAGGTT-3′, which produced a DNA fragment of 592 bp; GLUT7, 5′-CCCATGTACCTGGGAGAACTGG-3′ and 5′-ATCAGCTGCCAGCGCAGGGGCC-3′, which produced a DNA fragment of 390 bp; GLUT8, 5′-TGGCTGGCCGTGCTGGGCTGTG-3′ and 5′-AGTAGGTACCAAAGGCACTCAT-3′, which produced a DNA fragment of 464 bp; GLUT9, 5′-TTGAGCGCTTAGGAAGGAGACC-3′ and 5′-ACCGCTGCAGAACGAGGCAATG-3′, which produced a DNA fragment of 163 bp; GLUT10, 5′-AATGCCAGCCAGCAGGTGGATC-3′ and 5′-AGGACAGCGGTCAGCCCATAGA-3′, which produced a DNA fragment of 526 bp; GLUT12, 5′-GTGCTTAGTGAGATCTTTCCC-3′ and 5′-CCTTTGCTAGCTCCACTGATAT-3′, which produced a DNA fragment of 244 bp; and HMIT, 5′-CTGAAATCTATCCTCTCTGGGC-3′ and 5′-CAATGTACCTCCCTTCATCCGA-3′, which produced a DNA fragment of 284 bp. Analysis of DNA fragments was performed using agarose gel electrophoresis (1.5% agarose in TAE Buffer). Bands were visualized with ethidium bromide staining under UV light on a Fujifilm LAS-3000, and gels were analyzed using Fujifilm Multigauge 3.0 software.

Quantitative Reverse Transcriptase-PCR—Total RNA was isolated from bEnd.3 cells as described above, and quantitative RT-PCR was performed using an iScript One-Step RT-PCR kit With SYBR Green (Bio-Rad). Each reaction was run in duplicate using the following primers (IDT): GLUT1, 5′-AGCCCTGCTACAGTGTAT-3′ and 5′-AGGTCTCGGGTCACATC-3′, which generated a DNA fragment of 135 bp; GLUT8, 5′-TGTGGGCATAATCCAGGT-3′ and 5′-GGGTCAGTTTGAAGTAGGTAC-3′, which produced a DNA fragment of 140 bp; GLUT9, 5′-CTCATTGTGGGACGGTT-3′ and 5′-CAGATGAAGATGGCAGT-3′, which produced a DNA fragment of 132 bp, and as a mouse expression control, EIF1α, 5′-CAACA-

TCGTCGTAATCGGACA-3′ and 5′-GCTTAAGACCCAGG-CGTACTT-3′, which was used to normalize PCR data (29). Samples were run on an MJ Research PTC-200 Peltier Thermal Cycler with a Chromo4 real time PCR detector using Opticon Monitor 3 software (Bio-Rad). All primers were verified using One-Step RT-PCR kit (Qiagen) and run on a 2% agarose gel in TAE. Bands were visualized by ethidium bromide staining under UV light on a Fujifilm LAS-3000, and gels were analyzed using Fujifilm Multigauge 3.0 software.

bEnd.3 Cell ATP Depletion—Confluent bEnd.3 cells in 12-well dishes were washed twice with DPBS and incubated with DPBS + 5 mM glucose, DPBS + glucose + 5 mM KCN, or DPBS + glucose + 8 μg/ml FCCP for various intervals. Cells were processed and assayed using a Calbiochem luciferin-luciferase-based ATP assay kit per the kit instructions. Luminescence measurements were made using a Turner Veritas microplate luminometer or a Turner 20/20″ single tube luminometer.

ATP Recovery of bEnd.3 Cells—Confluent bEnd.3 cells in 12-well dishes were washed twice with DPBS and treated with DPBS + 5 mM glucose, DPBS + glucose + 5 mM KCN, or DPBS + glucose + 8 μg/ml FCCP for 10 min at 37 °C. The media were aspirated and replaced with normal cell growth media (DMEM + fetal bovine serum + penicillin/streptomycin). Cells were placed at 37 °C in normal growth media and incubated for various times. Cell processing and ATP measurements were performed as per the kit instructions.

Zero-trans Sugar Uptake Measurements—Confluent 150-cm^2 dishes of bEnd.3 cells were split into 12-well plates the afternoon before each experiment. On the day of the assay, cells were placed in serum-free DMEM for 2 h at 37 °C. Plates for AMPK activation measurements were treated with 2 mM of AICAR (Fisher) in serum-free DMEM for 2 h at 37 °C. Cells were washed with 1 ml of either DPBS or DPBS containing 5 mM KCN or 8 μg/ml FCCP and containing or lacking 5 mM glucose. Cells were incubated in 0.5 ml of wash media for 10 min at 37 °C and then placed on ice to cool in glucose-free medium. Incubation on ice for 10–15 min depletes intracellular sugar levels (via export) without changing cytoplasmic ATP levels. Wash medium was drained, and cells were treated with 400 μl of increasing concentrations of 3-*O*-methylglucose (3-OMG) containing 2.5 μCi/ml 3-*O*-[^{3}H] methylglucose (3-[^{3}H]OMG) in DPBS in the absence and present of the appropriate poison (KCN, FCCP, or AICAR). Uptake proceeded for 15 s at 5 and 10 mM 3-OMG and for 30 s at 20 and 40 mM 3-OMG. Uptake was stopped by adding 1 ml of uptake stop solution, and the media were immediately aspirated. Each well was washed two more times with 1 ml of stop solution and treated with 0.5 ml of Cell Lysis Buffer. Samples were counted in duplicate by liquid scintillation spectrometry (Beckman). Each measurement was performed in triplicate. Protein concentrations for each sample were determined using BCA protein assay kit (Pierce).

Cytochalasin B Inhibition of Sugar Uptake Measurements—Transport measurements were performed as above with the following modifications. Cells were serum-depleted in DMEM containing 25 mM glucose for 2 h prior to measuring uptake, washed with 1.5 ml DPBS, and allowed to incubate at 37 °C for 15 min. Plates were maintained at 37 °C throughout the

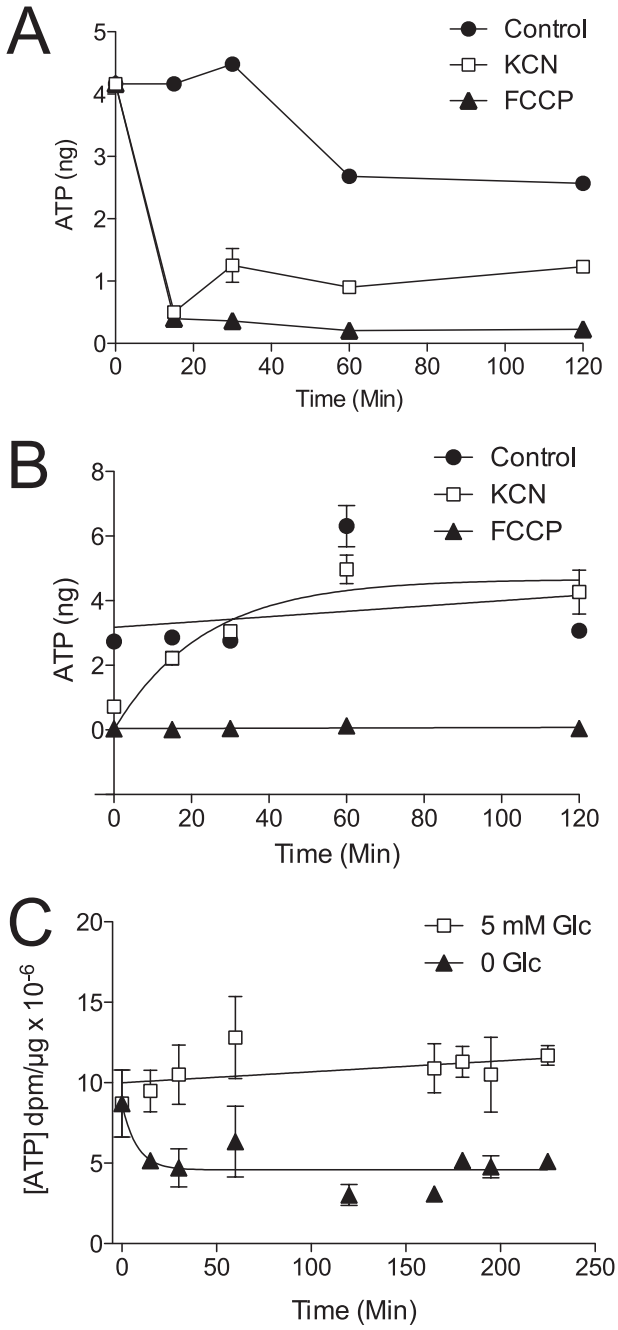

FIGURE 1. **ATP depletion in bEnd.3 cells.** *A,* time course of ATP depletion of bEnd.3 cells incubated with PBS containing 5 mM glucose (●), 5 mM glucose + 5 mM KCN (□), or 5 mM glucose + 8 μg/ml FCCP (▲). *Ordinate*, ATP levels in nanograms per 100 μl of cell extract. *Abscissa*, time of cellular exposure to poison in minutes. Data points represent the mean ± S.E. for three ATP assays. *B,* time course of ATP recovery following poisoning. Cells were treated with PBS containing 5 mM glucose (●), 5 mM glucose + 5 mM KCN (□), or 5 mM glucose + 8 μg/ml FCCP (▲) for 10 min and then restored to normal growth media (PBS plus 5 mM glucose) for the times indicated. *Ordinate,* ATP levels in nanograms per 100 μl of extract. *Abscissa*, time (minutes) that cells were allowed to recover from initial poisoning. Data points represent the mean ± S.E. for three separate ATP assays. *C,* time course of glucose depletion-induced ATP-depletion in bEnd.3 cells. Cells were treated with PBS containing 5 mM glucose (□) or 0 glucose (▲) for 0–230 min at 37 °C. *Ordinate*, ATP levels in dpm/μg total lysate protein. *Abscissa*, time (minutes) that cells were exposed to 0 or 5 mM glucose. Data points represent the mean ± S.E. for three separate ATP assays.

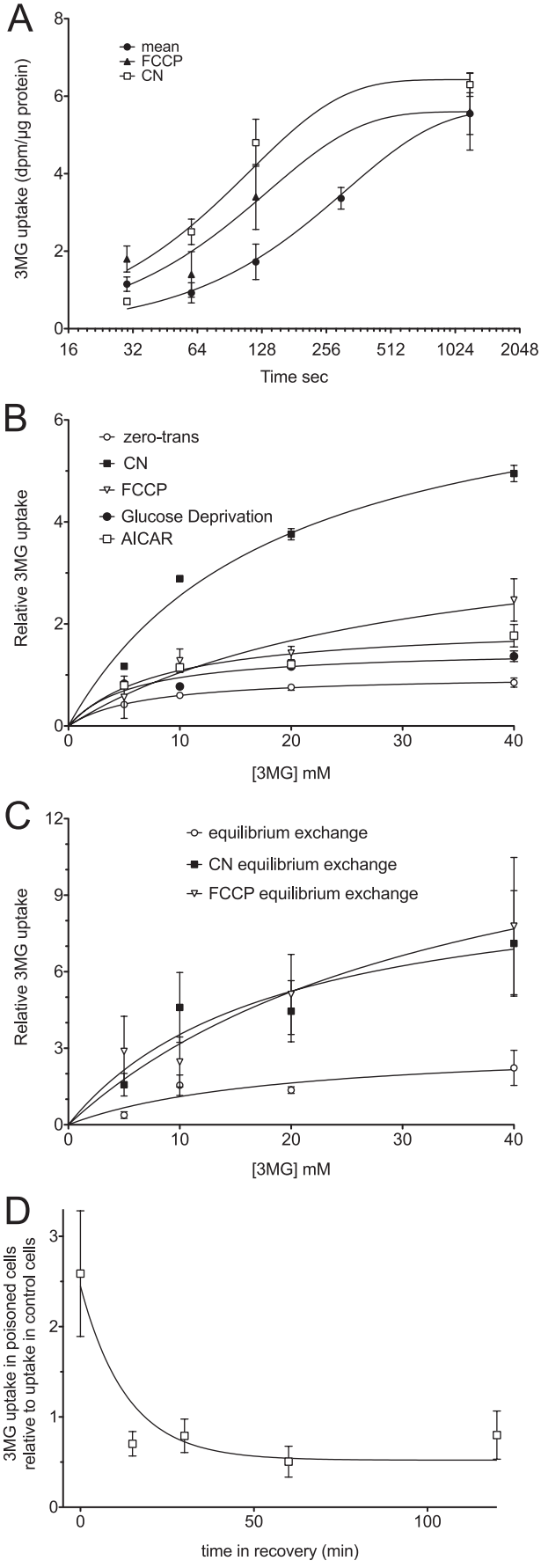

transport measurements. Uptake solutions consisted of 100 μM 2-deoxy-D-glucose with 2.5 μCi of 2-[^{3}H]deoxyglucose plus increasing concentrations of cytochalasin B from 0.1 to 10 μM. Uptake proceeded for 5 min, at which time uptake was stopped and the cells were washed and processed as described previously.

Equilibrium Exchange Sugar Uptake Measurements—In these experiments, intracellular concentrations of 3-OMG are equal to extracellular 3-OMG; therefore, transport is measured using 3-[^{3}H]OMG. Transport measurements were similar to zero-trans uptake measurements with the following modifications. Cells were serum-depleted in DMEM containing 5, 10, 20, or 40 mM 3-OMG for 2 h. Cells were washed and incubated as described previously with wash media containing 5, 10, 20, or 40 mM 3-OMG in DPBS, DPBS with 5 mM KCN, or DPBS with 8 μg/ml FCCP. Uptake was measured and terminated as described previously. Cells were then washed and processed as above.

Analysis of Sugar Uptake—All data analysis was performed using Synergy Software Kaleidagraph, version 4.0.

For zero-trans and equilibrium exchange transport experiments, background counts were subtracted and uptake, v, was normalized to total protein/well. Sugar uptake data were fitted to the Michaelis-Menten Equation 1,

$$v = \frac{V_{max}[S]}{K_m + [S]} \qquad \text{(Eq. 1)}$$

by nonlinear regression, and V_{max} and K_m values were extracted

FIGURE 2. **Sugar uptake at 4 °C in bEnd.3 cells.** *A,* time course of 20 mM 3-OMG uptake in control cells (●) or in cells exposed to 5 mM KCN (□) or to 8 μg/ml FCCP (▲) for 15 min at 37 °C prior to cooling, glucose depletion, and transport initiation. *Ordinate,* 3-OMG uptake (dpm per μg total cell protein); *abscissa*, time in seconds (note the log2 scale). Data points represent the mean ± S.E. of three separate determinations. The *curves* drawn through the points were computed by nonlinear regression assuming monoexponential 3-OMG uptake and have the following constants: *control*, equilibrium space = 5.65 ± 0.38 dpm/μg; k = 0.0032 ± 0.0005/s. For FCCP, equilibrium space = 5.60 ± 0.53 dpm/μg, k = 0.0073 ± 0.0017/s. For KCN, equilibrium space = 6.43 ± 0.58 dpm/μg, k = 0.0089 ± 0.0019/s. *B,* concentration dependence of zero-trans 3-OMG uptake in control cells (○), cells exposed to 5 mM KCN (■), 8 μg/ml FCCP (▽), 0 glucose (●), or to 2 mM AICAR (□) for 15 min at 37 °C. *Ordinate,* relative rate of unidirectional 3-OMG uptake; *abscissa*, [3-OMG] in millimolar. Prior to 30-s measurements of uptake, cells were cooled to 4 °C and incubated in 0-glucose medium for 15 min (sufficient time for intracellular glucose to become depleted through export). The *curves* were computed by nonlinear regression assuming that uptake is described by the Michaelis-Menten equation (Equation 1), and the resulting V_{max} and $K_{m(app)}$ values are summarized in Table 1. Each point represents the mean ± S.E. of three to eight separate experiments. *C,* equilibrium exchange transport. Cells were pre-loaded with increasing amounts of 3-OMG (from 5 to 40 mM) and allowed to equilibrate before treating for 10 min with control medium (○), 5 mM KCN (■), or 8 μg/ml FCCP (▽) each containing the preloading [3-OMG] at 37 °C. The cells were cooled, and unidirectional 3-OMG uptake was measured at 4 °C. *Ordinate* and *abscissa* are same as in *B*. The *curves* were computed by nonlinear regression assuming transport is described by Equation 1, and the resulting V_{max} and $K_{m(app)}$ values are summarized in Table 1. Each point represents the mean ± S.E. for three separate experiments. *D,* time course of recovery of KCN stimulation of transport upon washout of KCN. Cells were treated with 5 mM KCN for 15 min at 37 °C. The medium was then replaced with KCN-free medium containing glucose for the times shown on the *abscissa*. The cells were cooled to 4 °C and incubated in 0-glucose medium for 15 min (sufficient time or intracellular glucose to become depleted through export), and zero-trans 3-OMG uptake was measured at 20 mM 3-OMG. The *curve* drawn through the points was calculated by nonlinear regression assuming a monoexponential decay in transport rates. Transport falls 4-fold with a half-time of 9 min. Each point represents the mean ± S.E. of three separate experiments.

TABLE 1
Summary of 3-OMG transport in bEnd.3 cells

	Zero-trans uptake[a]					Equilibrium exchange uptake[b]				
	K_m[c]	95% confidence intervals[c]	Relative V_{max}[c]	95% confidence intervals[c]	n[d]	K_m	95% confidence intervals[c]	Relative V_{max}[c]	95% confidence intervals[c]	n[d]
Control	6.7 ± 0.4	5.1 to 8.4	1	0.9 to 1.1	12	14.9 ± 12.6	−62.2 to 99.9	3.17 ± 0.46[e]	−3.1 to 9.5	3
CN	18.7 ± 6.7	−10.5 to 47.9	7.32 ± 1.2[e,f]	2.1 to 12.6	6	18.4 ± 13.9	−41.4 to 78.3	10.0 ± 3.5[e]	−4.8 to 24.9	3
FCCP	30.1 ± 18.4	−48.9 to 109.2	4.26 ± 1.4	−1.8 to 10.2	6	35.9 ± 27.8	−83.9 to 155.8	14.6 ± 6.5[e]	−13.5 to 42.6	3
Glucose deprivation	29.4 ± 11.0	−8.6 to 20.5	1.7 ± 0.3[e]	0.5 to 2.7	3					
AICAR	8.4 ± 4.0	−8.8 to 25.7	2.0 ± 0.3[e]	0.6 to 3.4	4					

[a] Unidirectional sugar uptake into cells was depleted of sugar at 4 °C for 15 min.
[b] Unidirectional sugar uptake was into cells where $[3\text{-OMG}]_i = [3\text{-OMG}]_o$.
[c] The concentration dependence of sugar uptake was analyzed by nonlinear regression assuming Michaelis-Menten kinetics to obtain K_m and V_{max}. All V_{max} values are expressed relative to V_{max} for zero-trans uptake in matched control cells. Control zero-trans 3-OMG uptake V_{max} = 180 pmol/μg/min. Results are shown as mean ± S.E., and the 95% confidence intervals for the analysis are indicated.
[d] Number of separate experiments in which 3-OMG transport was measured was at least four different [3-OMG].
[e] V_{max} is significantly greater than control V_{max} for zero-trans uptake ($p < 0.05$).
[f] CN stimulation of V_{max} for 3-OMG zero-trans uptake is 3.18 ± 0.92-fold greater than FCCP stimulation of uptake.

from the fits. For cytochalasin B inhibition experiments, sugar uptake data were fitted to Equation 2,

$$\text{uptake} = \text{leakage} + \text{transport} - \frac{\text{transport}}{1 + \frac{[\text{CCB}]}{k_i}} \quad \text{(Eq. 2)}$$

and the inhibition constant (K_i) for cytochalasin B inhibition of transport was extracted from the fit.

Western Blotting of bEnd.3 Cells—Confluent 100-mm dishes of bEnd.3 cells were washed with DPBS and incubated in the absence or presence of 5 mM KCN or 8 μg/ml FCCP for 10 min, incubated in the absence of 5 mM glucose for 30 min, or incubated in the presence of 2 mM AICAR for 2 h as outlined previously. Cells were then washed twice with DPBS, lysed, and analyzed for total protein concentration using a micro BCA kit (Pierce). Lysates were normalized for total protein and run on either 4–12% BisTris or 10% BisTris gels in MES Buffer (Invitrogen), transferred to polyvinylidene difluoride membranes (ThermoFisher), blocked with either 5 or 10% bovine serum albumin, and probed with either 1:10,000 dilution of C-terminal antibody, a 1:5,000 dilution of mouse Na^+,K^+-ATPase antibody, or a 1:1,000 dilution of rabbit AMPK or AMPK (Thr(P)-172) antibody. A 1:30,000 dilution of either horseradish peroxidase-conjugated goat anti-rabbit or goat anti-mouse secondary antibody was also used (Jackson ImmunoResearch Laboratories). Chemiluminescence was visualized either on film or using the Fujifilm LAS-3000 with SuperSignal Reagent (Pierce). Band densities were quantitated using ImageJ software.

Biotinylation of bEnd.3 Cells—150-cm^2 plates of confluent bEnd.3 cells were washed twice with 25 ml of DPBS and incubated with 25 ml of either DPBS alone or DPBS containing 5 mM KCN or 8 μg/ml FCCP for 10 min at 37 °C. Plates were washed twice with ice-cold DPBS and incubated on ice in 12 ml of DPBS containing 1 mM EZ-Link Sulfo-NHS-SS-Biotin for 30 min with gentle rocking. The reaction was quenched with 2 ml of biotin quench solution. Cells were gently scraped into solution, washed with TBS, and pelleted. After washing a second time with TBS, cells were resuspended in Biotin Lysis Buffer, and biotinylated proteins were incubated with streptavidin beads in the absence or presence of 10,000 units (20 μl) of peptide:*N*-glycosidase F (New England Biolabs) at 37 °C for 1 h. Lysates were then processed per kit instructions. Protein concentrations were determined using bovine serum albumin as a standard. Samples were normalized for total protein and analyzed by Western blot.

RESULTS

ATP Depletion of bEnd.3 Cells—ATP levels were measured in bEnd.3 cells treated with PBS containing 5 mM glucose in the absence and presence of either 5 mM KCN or 8 μg/ml FCCP for up to 2 h (Fig. 1*A*). Although ATP depletion occurs within the first 15 min of treatment with both poisons, ATP levels in KCN-treated cells show a small bounce by 30 min and then remain stable. ATP levels in FCCP-treated cells are rapidly depleted and remain low throughout the time course. The effects of poisons are dose-dependent with half-maximal effects observed at 3 μM KCN and 0.25 ng/ml FCCP (Fig. 3, *A* and *C*).

We next examined the time course of ATP recovery following treatment with KCN and FCCP (Fig. 1*B*). bEnd.3 cells were poisoned for 10 min; the media were replaced with normal cell growth media, and the cells were sampled for ATP assays for up to 2 h post-poisoning (Fig. 1*B*). KCN washout allows cells to recover normal ATP levels within 60 min. ATP levels in FCCP-treated cells do not recover. Removal of extracellular glucose rapidly decreases cytoplasmic [ATP] by 50% (Fig. 1*C*).

Zero-trans Sugar Uptake—We next asked whether bEnd.3 cell ATP depletion affects sugar uptake. 3-OMG is a nonmetabolizable transport substrate. Sugar uptake at 10 mM 3-OMG and 4 °C shows simple monoexponential kinetics with a half-time of ~4 min (Fig. 2*A*). ATP depletion with FCCP (10 min at 8 μg/ml) or KCN (10 min at 5 mM) reduces the half-time for uptake to 2 and 1 min, respectively (Fig. 2*A*). The equilibrium 3-OMG space of the cells is not significantly affected by metabolic depletion indicating that poisons do not alter cell volume. The rate of sugar uptake in control and poisoned cells is inhibited by 84 ± 16% by the sugar transport inhibitor cytochalasin B with K_i = 122 ± 47 nM (n = 3) indicating that sugar import is protein-mediated.

V_{max} and K_m values for 3-OMG transport were obtained by nonlinear regression analysis of the concentration dependence of sugar uptake assuming that uptake is described by the Michaelis-Menten equation. Control bEnd.3 cell zero-trans 3-OMG uptake is characterized by a V_{max} of 180 ± 10

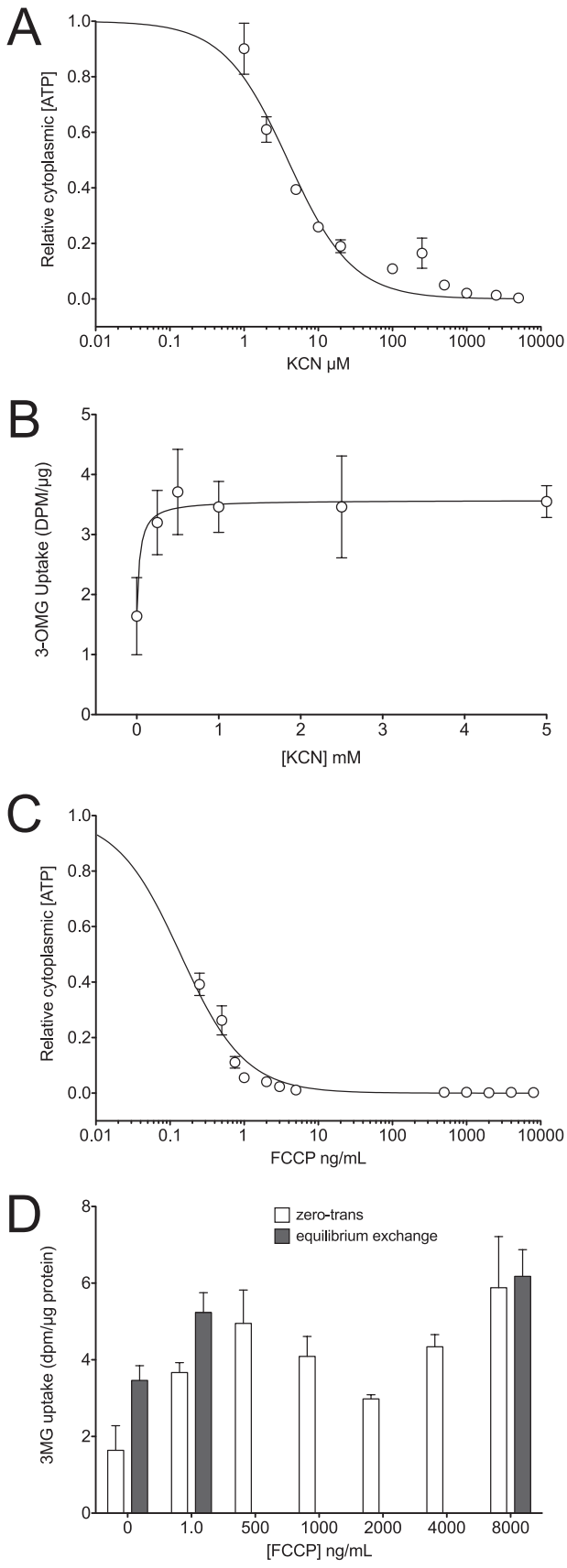

FIGURE 3. **Concentration dependence of ATP depletion (*A*) and transport stimulation (*B*) by KCN or concentration dependence of ATP depletion (*C*) and transport stimulation (*D*) by FCCP.** Cells were exposed to varying [poison] for 10 min at 37 °C and then cooled, and cellular ATP content was measured as described previously. *A* and *C, ordinates*, relative to cytoplasmic [ATP] (luminescence per unit of cell protein); *A* and *C, abscissas*, [poison]. *B* and *D, ordinates*, 3-OMG uptake in dpm/μg protein; *B* and *D, abscissas*, [poison]. Each experiment was repeated at least three times, and results are shown as mean ± S.E. *Curves* in *A* and *C* were computed assuming that [ATP] decreases in a saturable manner with [poison]. $K_{0.5}$ for [ATP] depletion by KCN <3.9 ± 0.6 μM and by FCCP is 0.14 ± 0.01 ng/ml. The *curve* in *B* was computed by nonlinear regression assuming that sugar uptake increases in a saturable manner with [poison]. $K_{0.5}$ for transport stimulation by KCN is 0.04 ± 0.03 mM. *D*, FCCP stimulation of zero-trans (*open bars*) and equilibrium exchange (*shaded bars*) transport are shown.

pmol/μg total cell protein/min and $K_{m(app)}$ of 6.7 ± 0.4 mM (Fig. 2*B*; Table 1). KCN and FCCP increase V_{max} for 3-OMG uptake by 7.2 ± 1.2- and 4.3 ± 1.4-fold, respectively. K_m for zero-trans 3-OMG uptake increases in metabolically stressed cells. Transport stimulation by KCN is rapidly reversed upon washout of KCN at 37 °C (Fig. 2*D*).

Equilibrium Exchange 3-OMG Uptake—Under physiological conditions, endothelial cells are bathed in serum and interstitial glucose and therefore rarely experience situations where intracellular glucose is zero. We therefore sought to measure sugar uptake in bEnd.3 cells under equilibrium exchange conditions that more closely resemble those experienced *in vivo*. In equilibrium exchange, the concentrations of intracellular and extracellular 3-OMG are identical, and unidirectional sugar transport is measured using 3-[^{3}H]OMG. Equilibrium exchange 3-OMG uptake was measured in the absence and presence of either 5 mM KCN or 8 μg/ml FCCP (Fig. 2*C*). Equilibrium 3-OMG uptake in control cells is characterized by a V_{max} of 571 ± 83 pmol/μg total cell protein/min and $K_{m(app)}$ of 14.9 ± 12.6 mM (Fig. 2*C*; Table 1). This suggests that as with transport in erythrocytes, unidirectional sugar uptake displays trans-acceleration (19). KCN and FCCP increase V_{max} for exchange 3-OMG uptake by 3.2 ± 1.1- and 4.6 ± 2.1-fold, respectively. Poisoning has no significant affect on K_m for exchange 3-OMG uptake.

KCN and FCCP depletion of cellular [ATP] (Fig. 3, *A* and *C*) and stimulation of 3-OMG uptake (Fig. 3, *B* and *D*) are dose-dependent with $K_{0.5}$ for transport stimulation of 0.04 ± 0.03 mM KCN and <1 ng/ml FCCP. Zero-trans and exchange 3-OMG transport are equally sensitive to FCCP (Fig. 3*D*).

Quantitation of GLUT1 mRNA Using RT-PCR—To examine whether increases in zero-trans and equilibrium exchange sugar transport capacity are caused by up-regulation of GLUT1 expression (or any other GLUT), we first measured bEnd.3 GLUT1 mRNA levels using end point RT-PCR in the absence and presence of either 5 mM KCN or 8 μg/ml FCCP. At the same time, we screened for the presence of mRNA for the other GLUT family members known to exist in mice. Although end point RT-PCR is not quantitative, the primer sets and total mRNA template concentrations used for each sample were the same. Our results obtained indicate that there are no changes in total GLUT1 mRNA levels in the presence of either KCN or FCCP (Fig. 4, *A* and *B*), and the summary of GLUT mRNA levels detected can be found in Table 2. Interestingly, mRNA for the class 3 transporter GLUT8 and the class 2 transporter GLUT9 was detected by end point RT-PCR.

To obtain a more quantitative analysis, we used quantitative RT-PCR to probe for changes in GLUT1, GLUT8, and GLUT9

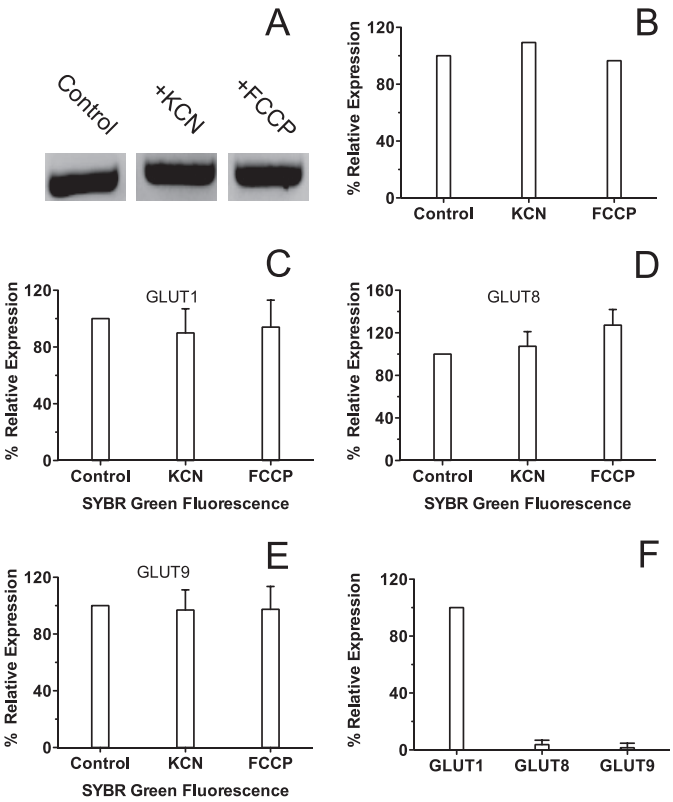

FIGURE 4. **RT-PCR of bEnd.3 cells.** *A,* end point reverse transcriptase-PCR of bEnd.3 cells using a GLUT1 primer. Cells were incubated for 10 min in either PBS, PBS + 5 mM KCN, or PBS + 8 μg/ml FCCP before isolating total RNA, and reverse transcriptase-PCR was carried out using a GLUT1 primer. Samples were run on a 1.5% agarose gel. *B,* quantitation of GLUT1 band densities from end point RT-PCR. *Ordinate*, relative expression (%). Experimental conditions (control PBS, PBS + KCN, and PBS + FCCP) are shown *below* the *abscissa*. *C–F,* quantitative RT-PCR of bEnd.3 cells. *Ordinate* and *abscissa* are as in *B*. Cells were processed as in *A* and 100 ng of total RNA was used for each reaction, which was run twice with four replicates for each condition. Results are shown as mean ± S.E. Primers specific to GLUT1 (*C*), GLUT8 (*D*), and GLUT9 (*E*) were used in each reaction. *F,* in this *chart,* the amount of GLUT8 and GLUT9 message in control cells is expressed relative to GLUT1 message in control cells.

mRNA levels in the presence of 5 mM KCN or 8 μg/ml FCCP. Four separate mRNA samples were prepared in the absence or presence of either 5 mM KCN or 8 μg/ml FCCP, and each template was used to run the quantitative RT-PCR. The results were analyzed using the ΔΔ*Ct* method, averaged, and compared for relative mRNA expression. As with the end point RT-PCR, our results show no significant change in GLUT1, GLUT8, or GLUT9 mRNA levels during KCN- or FCCP-induced ATP depletion (Fig. 4, *C–E*). Analysis of relative expression levels of the detected GLUT mRNA shows that GLUT1 message is at least 33-fold higher than either GLUT8 or GLUT9 in bEnd.3 cells (Fig. 4*F*).

Plasma Membrane Biotinylation of bEnd.3 GLUT1—ATP depletion of bEnd.3 cells does not alter GLUT1 message levels. However, increased translation of presynthesized GLUT1 mRNA could increase levels of plasma membrane resident protein, resulting in increased zero-trans and exchange sugar transport capacity. To test for this possibility, cells were incubated for 10 min in the absence or presence of 5 mM KCN or 8 μg/ml FCCP, lysed, and analyzed by Western blot (Fig. 5*A*). Two GLUT1 C-terminal antibody reactive bands are observed as follows: a 48-kDa species and a more abundant and broadly

TABLE 2
GLUT mRNA levels detected by end point RT-PCR
Analysis of bEnd.3 cell GLUTs was by end point RT-PCR.

Transporter[a]	Class[b]	mRNA detected[c]
Glut1	1	Yes
Glut2	1	No
Glut3	1	No
Glut4	1	No
Glut5	2	No
Glut6	3	No
Glut7	2	No
Glut8	3	Yes
Glut9	2	Yes
Glut10	3	No
Glut11	2	NA[d]
Glut12	3	No
HMIT (*Glut13*)	3	No
Glut14	1	NA[d]

[a] Transporter indicates the glucose transporter isoform tested.
[b] Class indicates the glucose transport class (1, 2, or 3) to which the GLUT isoform belongs.
[c] Was GLUT RNA detected?
[d] *Glut11* and *Glut14* genes have not been detected in mouse to date.

mobile species of 55 kDa. Treatment of membranes with peptide:*N*-glycosidase F causes both species to collapse to a 42-kDa GLUT1 C-terminal antibody-reactive species (see supplemental Fig. 1). Densitometric analysis indicates that neither the 48- nor the 55-kDa species is significantly increased by KCN or FCCP. This result combined with the quantitative RT-PCR results indicates that increases in zero-trans and exchange V_{max} are not explained by either increased GLUT1 message or protein in bEnd.3 cells.

We next asked whether cell surface recruitment of intracellular GLUT1 was responsible for increased sugar transport. Cells were incubated for 10 min in PBS in the absence or presence of 5 mM KCN or 8 μg/ml FCCP, washed, and then cooled to 4 °C. Cells were then treated with a membrane-impermeable, amine-reactive biotin (sulfo-NHS-SS-biotin), and the reaction was quenched, and the cells were lysed in detergent-containing Lysis Buffer. Biotinylated proteins were precipitated with streptavidin beads and analyzed by Western blot (Fig. 5, *C* and *E*), and band densities were quantitated (Fig. 5, *D* and *F*). The blots indicate that ATP depletion of bEnd.3 cells increases cell surface GLUT1 C-terminal antibody-reactive species by at least 2-fold, whereas surface Na^+,K^+-ATPase levels are unaffected by metabolic stress. Interestingly, cell surface expression of the 48-kDa GLUT1 C-terminal antibody-reactive species is unchanged by metabolic depletion, whereas expression of the 55-kDa species is increased by 3–5-fold (Fig. 5, *C* and *D*). These results mirror the 2–7-fold increase in 3-OMG transport capacity produced by metabolic poisons.

AMPK is a key regulator of cellular glucose transport and glycolysis in muscle and heart (30, 31). AICAR (an AMPK agonist) enters cells via nucleoside transporters, is transformed to 5-aminoimidazole-4-carboxamide riboside monophosphate (ZMP), and then allosterically activates AMPK (32). AICAR (2 mM) treatment of bEND.3 cells for 2 h increases V_{max} for zero-trans 3-OMG uptake (Fig. 2*B*; Table 1). Glucose depletion, KCN, FCCP, or AICAR treatment of bEnd.3 cells increases AMPK phosphorylation as judged by immunoblot analyses using AMPK and phospho-AMPK-directed antibodies (Fig. 6).

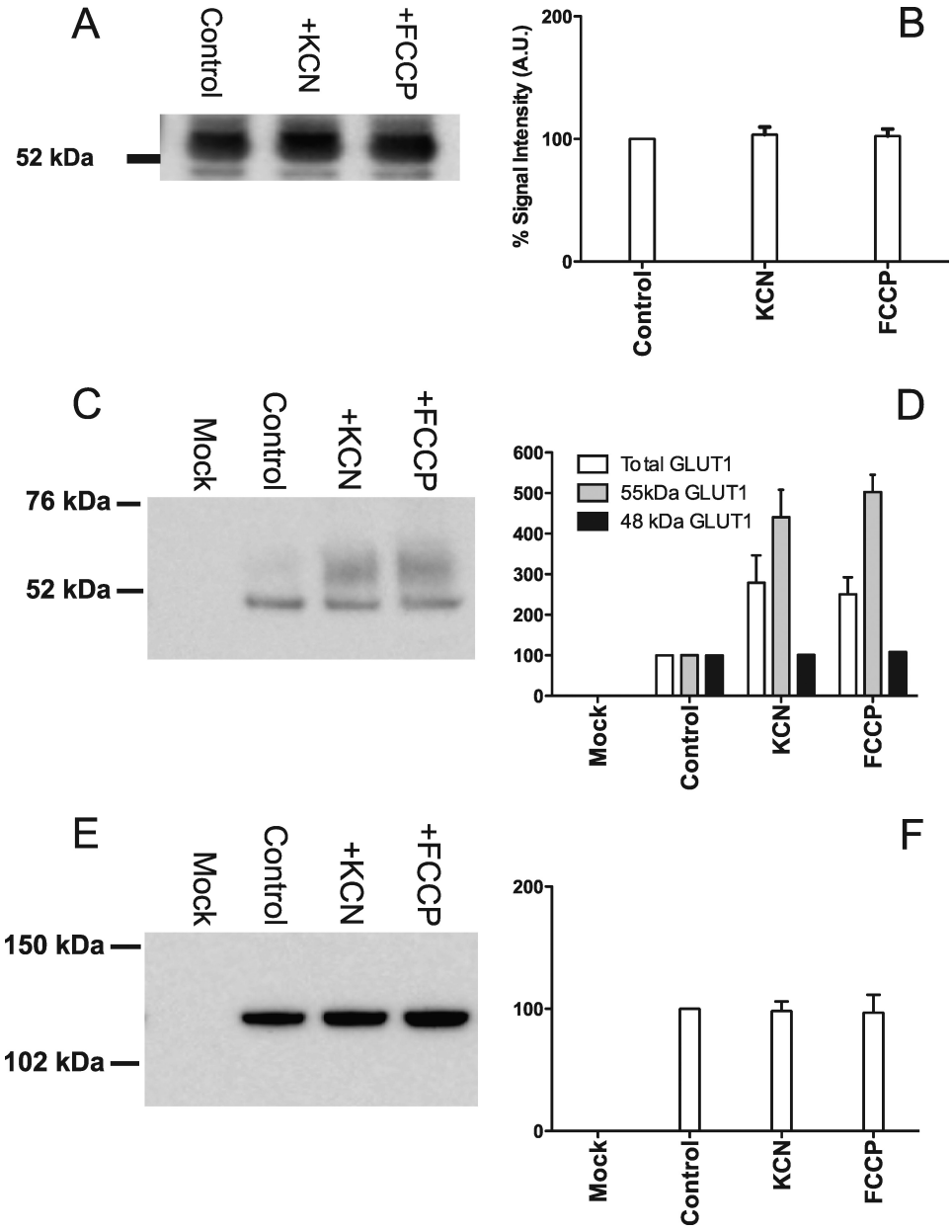

FIGURE 5. **Biotinylation of bEnd.3 cell surface proteins.** *A,* representative Western blot of whole cell lysates of bEnd.3 cells in the absence or presence of either 5 mM KCN or 8 μg/ml of FCCP for 10 min. Total protein (20 μg) was loaded into each lane and probed with GLUT1 C-terminal antibody. *B,* quantitation of Western blot band density. *Ordinate*, relative expression (%); *abscissa*, experimental condition −PBS, PBS + KCN, and PBS + FCCP. *C* and *E,* representative Western blots of cell surface biotinylated bEnd.3 cell proteins obtained in the absence and presence of either 5 mM KCN or 8 μg/ml FCCP. Cells were poisoned at 37 °C for 10 min before cooling to 4 °C and biotinylation. 30 μg of total streptavidin-pulldown protein was loaded onto each gel and blotted with either GLUT1 C-terminal antibody (*C*) or antibody raised against Na^+,K^+-ATPase (*E*). Band densities were quantitated and shown in *D* (GLUT1) and *F* (Na^+,K^+-ATPase). *Ordinate* and *abscissa* are as in *B*. *D*, results are shown for total C-terminal antibody-reactive species (*open bars*), for 55-kDa C-terminal antibody-reactive species (*gray bars*), and for 48-kDa C-terminal antibody-reactive species (*black bars*). Each experiment was repeated at least three times, and the results of quantitations (*B, D,* and *F*) are shown as mean ± S.E.

DISCUSSION

This study examines the hypothesis that brain microvasculature endothelial cells respond acutely to cellular metabolic stress with increased sugar transport capacity resulting from recruitment of intracellular GLUT1 stores to the plasma membrane.

Previous studies have used the metabolic poisons KCN and FCCP to induce acute metabolic stress in cardiomyocytes, skeletal muscle, and nucleated erythrocytes (33–35). Metabolic depletion rapidly stimulates sugar transport in these tissues (33–35). In this study, we demonstrate rapid depletion of ATP in bEnd.3 cells using metabolic poisons. ATP levels recover within 60 min of removal of KCN; however, the effect of FCCP treatment is irreversible. We also show that KCN or FCCP treatment induces a 3.2–7.2-fold increase in V_{max} for zero-trans and equilibrium exchange sugar uptake in bEnd.3 cells.

Acute glucose depletion (15 min at 37 °C) also rapidly reduces bEnd.3 cell ATP content but only by 50%. This treatment increases V_{max} for sugar uptake suggesting that sugar transport in blood-brain barrier endothelial cells is, like transport in cardiomyocytes and skeletal muscle, acutely sensitive to cellular metabolic status (31, 36). AMPK is a key regulator of cellular metabolism. Upon elevation of cytoplasmic AMP levels, AMPK is phosphorylated and acts as a metabolic master switch, stimulating important metabolic processes such as fatty acid oxidation and glycolysis (37, 38). Activated AMPK stimulates glycolysis in hypoxic cardiomyocytes and monocytes by activating 6-phosphofructo-2-kinase (30, 31). Activated AMPK further supports increased anaerobic metabolism in heart and skeletal muscle by promoting recruitment of GLUT4 and GLUT1 to the cell membrane (39, 40), thereby increasing sugar uptake and metabolism. This mechanism may also be active in brain microvasculature endothelial cells because bEnd.3 cells acutely respond to metabolic poison, glucose depletion, and to the AMPK agonist AICAR with increased AMPK phosphorylation as well as increased sugar transport rates.

Quantitative PCR and Western blot analyses of whole cell lysates show no significant changes in either GLUT1 mRNA levels or total protein expression in ATP-depleted cells. PCR data also indicate that GLUT1 appears to be the only GLUT isoform expressed at significant levels in bEnd.3 cells. Plasma membrane protein biotinylation studies show that GLUT1 levels are increased at the plasma membrane by 2–2.5-fold within 10 min of treatment with either KCN or FCCP. These findings suggest that metabolic depletion of brain micro-

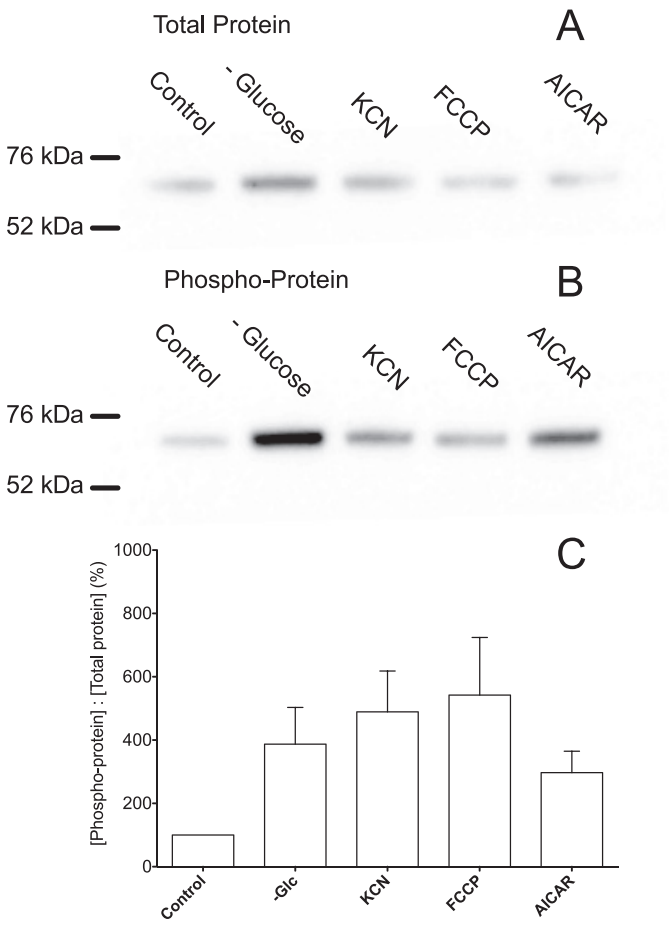

FIGURE 6. **Immunoblot analysis of bEnd.3 cell AMPK and phosphorylated AMPK content.** *A* and *B,* whole cell lysates (20 μg of protein) were resolved by SDS-PAGE and immunoblotted using AMPK (*A*) and phosphorylated AMPK (*B*)-directed antibodies. Prior to lysis, cells were treated for 15 min at 37 °C with 5 mM glucose (control), 0 glucose, 5 mM KCN, 8 μg/ml FCCP, or 2 mM AICAR. The mobilities of 76- and 52-kDa molecular mass standards are indicated. *C,* quantitation of band densities. *Ordinate,* ratio of immunoreactive phosphorylated AMPK to AMPK in extracts. *Abscissa,* experimental conditions (control PBS, 0 glucose, PBS + KCN, PBS + FCCP, and PBS + AICAR). Results are shown as mean ± S.E. of three separate experiments.

vasculature endothelial cells results in AMPK activation, which in turn may induce net GLUT1 translocation to the cell membrane.

Immunoblot analysis of the GLUT1 content of bEnd.3 cell total lysates and streptavidin pulldowns of biotinylated membrane proteins indicate that two GLUT1 C-terminal antibody-reactive species are present as follows: a minor 48-kDa protein and a more broadly mobile 55-kDa species. Both species collapse into a 42-kDa species upon treatment with the glycosidase peptide:*N*-glycosidase F suggesting that each corresponds to a differentially glycosylated form of GLUT1. Similar behavior is observed for human red cell GLUT1 (41, 42) and rat brain microvascular endothelial cells (43). Interestingly, cell surface levels of the 48-kDa species are unaffected by metabolic depletion, whereas surface levels of the 55-kDa species are significantly increased giving rise to an approximate 2–3-fold increase in total cell surface GLUT1.

It is interesting to compare our findings using cultured bEnd.3 cells with transport studies in polarized endothelial cells. Rat blood-brain barrier glucose transport is acutely stimulated during seizure, and immunohistochemical analysis suggests that this results from recruitment of intracellular GLUT1 to both luminal and abluminal endothelial cell membranes (44). This being the case, our demonstration of GLUT1 recruitment in an unpolarized endothelial cell is not only representative of recruitment in a polarized bEND cell *in vivo* but may also uniquely provide the tools for detailed biochemical analysis of this phenomenon.

Earlier immunohistochemical analyses of GLUT1 expression in rat bEND cells *in situ* suggesting an asymmetric (1:4) distribution of GLUT1 between luminal and abluminal membranes (45) appear to be incorrect. Rather, GLUT1 is equally distributed between luminal and abluminal membranes (8). If stimulation of trans-capillary transport involves GLUT1 recruitment to luminal and abluminal endothelial membranes, polarized GLUT1 expression in bEND cells would significantly impact net transport stimulation.

Our analysis (9, 46) indicates that starting from an equal distribution of carriers in luminal and abluminal membranes, increasing abluminal or luminal [GLUT1] in the absence of a commensurate increase at the trans-membrane would be without impact on net trans-endothelial cell sugar transport because the transport capacity of the membrane containing the fewest numbers of transporters remains rate-limiting. Polarized GLUT1 expression in the blood-brain barrier endothelium only makes sense if one membrane (*e.g.* the luminal membrane) contains many more transporters than the abluminal membrane and regulation involves up-regulation at the abluminal membrane. The available evidence argues against this (8).

In summary, acute metabolic depletion of murine bEnd.3 cells results in AMPK phosphorylation, GLUT1 recruitment to the cell membrane, and increased sugar transport. This may allow endothelial cells to respond rapidly with increased blood-brain barrier sugar transport in locally hypoxic or metabolically stressed regions of the brain. The exact nature of the involvement of AMPK in GLUT1 regulation in bEnd.3 cells requires further investigation.

REFERENCES

1. Flier, J. S., Mueckler, M., McCall, A. L., and Lodish, H. F. (1987) *J. Clin. Invest.* **79,** 657–661
2. Gerhart, D. Z., LeVasseur, R. J., Broderius, M. A., and Drewes, L. R. (1989) *J. Neurosci. Res.* **22,** 464–472
3. Kalaria, R. N., Gravina, S. A., Schmidley, J. W., Perry, G., and Harik, S. I. (1988) *Ann. Neurol.* **24,** 757–764
4. Pardridge, W. M., Boado, R. J., and Farrell, C. R. (1990) *J. Biol. Chem.* **265,** 18035–18040
5. Takata, K., Kasahara, T., Kasahara, M., Ezaki, O., and Hirano, H. (1990) *Biochem. Biophys. Res. Commun.* **173,** 67–73
6. Oldendorf, W. H., Cornford, M. E., and Brown, W. J. (1977) *Ann. Neurol.* **1,** 409–417
7. Coomber, B. L., and Stewart, P. A. (1985) *Microvasc. Res.* **30,** 99–115
8. Dejana, E. (2004) *Nat. Rev. Mol. Cell Biol.* **5,** 261–270
9. Simpson, I. A., Carruthers, A., and Vannucci, S. J. (2007) *J. Cereb. Blood Flow Metab.* **27,** 1766–1791
10. Harik, S. I., Behmand, R. A., and LaManna, J. C. (1994) *J. Appl. Physiol.* **77,** 896–901
11. McCall, A. L., Fixman, L. B., Fleming, N., Tornheim, K., Chick, W., and Ruderman, N. B. (1986) *Am. J. Physiol.* **251,** E442–E447
12. Kumagai, A. K., Kang, Y. S., Boado, R. J., and Pardridge, W. M. (1995) *Diabetes* **44,** 1399–1404

13. Simpson, I. A., Appel, N. M., Hokari, M., Oki, J., Holman, G. D., Maher, F., Koehler-Stec, E. M., Vannucci, S. J., and Smith, Q. R. (1999) *J. Neurochem.* **72,** 238–247
14. Pardridge, W. M. (1983) *Physiol. Rev.* **63,** 1481–1535
15. Cornford, E. M., Nguyen, E. V., and Landaw, E. M. (2000) *Am. J. Physiol. Heart Circ. Physiol.* **279,** H1346–H1354
16. Carruthers, A. (1986) *J. Biol. Chem.* **261,** 11028–11037
17. Hebert, D. N., and Carruthers, A. (1986) *J. Biol. Chem.* **261,** 10093–10099
18. Levine, K. B., Hamill, S., Cloherty, E. K., and Carruthers, A. (2001) *Blood Cells Mol. Dis.* **27,** 139–142
19. Levine, K. B., Cloherty, E. K., Hamill, S., and Carruthers, A. (2002) *Biochemistry* **41,** 12629–12638
20. Blodgett, D. M., De Zutter, J. K., Levine, K. B., Karim, P., and Carruthers, A. (2007) *J. Gen. Physiol.* **130,** 157–168
21. Boado, R. J. (1995) *Neurosci. Lett.* **197,** 179–182
22. Boado, R. J., Wu, D., and Windisch, M. (1999) *Neurosci. Res.* **34,** 217–224
23. Cornford, E. M., Hyman, S., and Pardridge, W. M. (1993) *J. Cereb. Blood Flow Metab.* **13,** 841–854
24. Farrell, C. L., and Pardridge, W. M. (1991) *Proc. Natl. Acad. Sci. U.S.A.* **88,** 5779–5783
25. Barros, L. F., Barnes, K., Ingram, J. C., Castro, J., Porras, O. H., and Baldwin, S. A. (2001) *Pflugers Arch.* **442,** 614–621
26. Sone, H., Deo, B. K., and Kumagai, A. K. (2000) *Invest. Ophthalmol. Vis. Sci.* **41,** 1876–1884
27. Omidi, Y., Campbell, L., Barar, J., Connell, D., Akhtar, S., and Gumbleton, M. (2003) *Brain Res.* **990,** 95–112
28. Souza-Menezes, J., Morales, M. M., Tukaye, D. N., Guggino, S. E., and Guggino, W. B. (2007) *Cell. Physiol. Biochem.* **20,** 455–464
29. Ohkawa, Y., Marfella, C. G., and Imbalzano, A. N. (2006) *EMBO J.* **25,** 490–501
30. Marsin, A. S., Bertrand, L., Rider, M. H., Deprez, J., Beauloye, C., Vincent, M. F., Van den Berghe, G., Carling, D., and Hue, L. (2000) *Curr. Biol.* **10,** 1247–1255
31. Marsin, A. S., Bouzin, C., Bertrand, L., and Hue, L. (2002) *J. Biol. Chem.* **277,** 30778–30783
32. Corton, J. M., Gillespie, J. G., Hawley, S. A., and Hardie, D. G. (1995) *Eur. J. Biochem.* **229,** 558–565
33. Haworth, R. A., and Berkoff, H. A. (1986) *Circ. Res.* **58,** 157–165
34. Hayashi, T., Wojtaszewski, J. F., and Goodyear, L. J. (1997) *Am. J. Physiol.* **273,** E1039–E1051
35. Simons, T. J. (1983) *J. Physiol.* **338,** 477–499
36. Coven, D. L., Hu, X., Cong, L., Bergeron, R., Shulman, G. I., Hardie, D. G., and Young, L. H. (2003) *Am. J. Physiol. Endocrinol. Metab.* **285,** E629–E636
37. Hardie, D. G. (2004) *Rev. Endocr. Metab. Disord.* **5,** 119–125
38. Hardie, D. G., Scott, J. W., Pan, D. A., and Hudson, E. R. (2003) *FEBS Lett.* **546,** 113–120
39. Barnes, K., Ingram, J. C., Porras, O. H., Barros, L. F., Hudson, E. R., Fryer, L. G., Foufelle, F., Carling, D., Hardie, D. G., and Baldwin, S. A. (2002) *J. Cell Sci.* **115,** 2433–2442
40. Mu, J., Brozinick, J. T., Jr., Valladares, O., Bucan, M., and Birnbaum, M. J. (2001) *Mol. Cell* **7,** 1085–1094
41. Gorga, F. R., Baldwin, S. A., and Lienhard, G. E. (1979) *Biochem. Biophys. Res. Commun.* **91,** 955–961
42. Vannucci, S. J., Maher, F., and Simpson, I. A. (1997) *Glia* **21,** 2–21
43. Kumagai, A. K., Dwyer, K. J., and Pardridge, W. M. (1994) *Biochim. Biophys. Acta* **1193,** 24–30
44. Cornford, E. M., Hyman, S., Cornford, M. E., Landaw, E. M., and Delgado-Escueta, A. V. (1998) *J. Cereb. Blood Flow Metab.* **18,** 26–42
45. Simpson, I. A., Vannucci, S. J., DeJoseph, M. R., and Hawkins, R. A. (2001) *J. Biol. Chem.* **276,** 12725–12729
46. Mangia, S., Simpson, I. A., Vannucci, S. J., and Carruthers, A. (2009) *J. Neurochem.* **109,** Suppl. 1, 55–62